European Journal of Technique

journal homepage: https://dergipark.org.tr/en/pub/ejt

Vol.16, No.1, 2026

Research Article

Experimental and ANOVA-Based Statistical Analysis of the Effects of Infill Pattern and Density on the Tensile Properties of FDM-Printed ABS, PETG, and PLA Thermoplastics

Ismail Erhan Kutsal[1], Serkan Bati[2*], Yahya Hisman Celik[3]

[1]Sirnak University, Sirnak Vocational School, Sirnak, Turkey. (e-mail: iekutsal@sirnak.edu.tr).
[2*] Batman University, Department of Mechanical Engineering, Batman, Turkey. (e-mail: serkan.bati@batman.edu.tr).
[3] Batman University, Department of Mechanical Engineering, Batman, Turkey. (e-mail: yahyahisman.celik@batman.edu.tr).

ARTICLE INFO

Received: Dec.,01.2026
Revised: Mar.,04.2026
Accepted: Mar.,24.2026

Keywords:
Fused deposition modeling
Additive manufacturing
Tensile strength
Modulus of elasticity
Elongation
ABS, PLA, PETG components
Analysis of variance

Corresponding author:

ISSN: *2536-5010* | e-ISSN: *2536-5134*

DOI: https://doi.org/10.36222/ejt.1833705

ABSTRACT

In this study, the effects of material type, infill pattern, and infill density on the tensile strength of ABS, PLA, and PETG specimens manufactured using the Fused Deposition Modeling (FDM) method were investigated. The effects of different infill patterns (linear, triangular, and honeycomb) and infill densities (15%, 30%, and 45%) on the mechanical properties were experimentally examined, and the obtained data were statistically analyzed using analysis of variance (ANOVA). The results indicated that mechanical performance generally increased with increasing infill density. According to the ANOVA results, filament type had a dominant effect on mechanical properties, contributing 83.64% to tensile strength, 54.95% to elongation, and 88.51% to the modulus of elasticity. The infill pattern showed a secondary effect on elongation (18.67%), whereas infill density exhibited secondary effects on tensile strength (8.89%) and modulus of elasticity (6.70%). Furthermore, specific strength and specific modulus values were calculated using the effective densities of the samples to evaluate performance per unit weight. Repeated ANOVA analyses revealed that the effect of infill density on specific tensile strength increased significantly to 28.17%, while no significant effect was observed on the specific modulus.

1. INTRODUCTION

The term additive manufacturing (AM), introduced in 1980s, is a method that facilitates the production of complex geometries with design flexibility, enables customized mechanical properties, and increases manufacturing freedom by allowing the use of a wide variety of materials in modern industrial applications [1,2]. Fused deposition modeling (FDM) remains one of the most common AM techniques and is also referred to as material extrusion 3D printing (ME3DP) or fused filament fabrication (FFF) [3,4].

FDM involves the melting of thermoplastic polymer filaments through a heating unit and the layer-by-layer deposition of material, enabling the production of highly accurate parts directly from digital models [5-7]. This method allows for the fabrication of high-strength components using low-cost polymers and provides rapid and efficient manufacturing, particularly for flexible or otherwise difficult-to-produce designs [8]. The most common thermoplastics in FDM are biodegradable (under certain conditions) and sustainable polylactic acid (PLA), lightweight and durable acrylonitrile butadiene styrene (ABS), and glycol-modified polyethylene terephthalate (PETG) [9,10]. Additionally, thermoplastics such as polyamide 6 (PA6), polypropylene (PP), polycarbonate (PC), and polyether ether ketone (PEEK) are employed in industrial applications [11].

Polymer products fabricated by FDM process are employed across various industries depending on the filament type and processing parameters. These applications include aviation and space industry, medical and biomedical fields [12], automotive and electronics [13], prototyping [1], small-scale mass production [14], as well as architectural and decorative artistic applications [15].

The mechanical performance, dimensional accuracy, and structural integrity of parts vary depending on the filament type and processing parameters. These parameters can be categorized into thermal conditions (nozzle and build plate temperatures, cooling rate), filament flow and printing speed, and geometric configurations (layer height, layer width, raster angle, infill density and pattern) [16, 17,18, 19].

Thermal conditions directly influence the melting of the filament, the bonding between deposited layers, and the overall thermal behavior. Key parameters include the nozzle temperature, build plate temperature, and cooling rate. The nozzle temperature determines the viscosity of the filament and the intermolecular fusion between successive layers. Increasing the nozzle temperature improves flow characteristics, enhancing interlayer bonding and thereby improving the mechanical properties. This effect has been shown to increase interfacial fracture toughness [12]. The build plate temperature is particularly critical for polymers with high melting points. Raising the bed temperature has been reported to enhance the tensile strength of materials printed with such polymers. In addition, the cooling rate and temperature affect the crystallinity of thermoplastic materials, thereby altering their final mechanical properties [20, 21].

Interlayer bonding time and void formation are determined by the interaction between filament deposition rate and quantity, as well as thermal conditions. High deposition rates can prevent the filament from achieving sufficient thermal fusion, leading to increased interlayer voids and consequently reduced tensile strength. The filament feed rate and flow volume can be optimized together with the deposition rate to minimize the porosity of printed parts [12].

Geometric settings also play a crucial role in determining the mechanical performance of FDM parts. These settings include layer height, layer width, raster angle/filament orientation, infill density, infill pattern, and nozzle geometry and diameter. Layer height is a critical factor affecting mechanical properties, void formation, and dimensional accuracy [22,23]. Reducing the layer height has been shown to increase tensile strength and reduce porosity in bio-composite specimens [12]. However, in PEEK/fiber-reinforced composites, increasing the layer height negatively impacts mechanical properties [24]. Gonabadi et al. [23] reported that layer height, layer width, and overlap region influence the size of inter-bead voids, which particularly reduce stiffness along with the thickness. Raster angle or filament orientation determines the deposition direction of the filament and is a key parameter for load transfer mechanisms [22].

The raster angle affects the tensile strength and the fracture behavior. For example, in PLA+ specimens, the highest maximum force and ultimate tensile strength were observed at a 90° raster angle, whereas a ±45° raster angle exhibited the greatest elongation and toughness [8]. Similarly, Kopar et al. [14] investigated the effect of print speed (60, 70, 80 mm/s) and raster angle (±45° and 0–90°) on the mechanical performance of ABS specimens produced via FFF. A tensile strength of 36.26 MPa was achieved at 60 mm/s and ±45°, while 31.77 MPa was recorded at 0–90°. Çakan [25] observed that increasing the raster angle reduces ultimate tensile strength, with maximum strength occurring at 0°. Faidallah et al. [26] reported that on-edge 0° orientation exhibited the highest tensile properties in PETG specimens with different standard geometries.

Infill density controls the amount of material in the inner layers and generally improves mechanical properties and interlayer bonding by reducing void content [27]. However, 100% infill density increases energy consumption [28]. Khan et al. [29], in a PLA-PETG-ABS composite study, reported that increasing infill density improves tensile strength. After layer height, infill density was found by Sagias et al. [2] to be the second most important factor influencing mechanical characteristics in ABS specimens. The infill pattern, which defines the internal structure, also influences strength and toughness; Galeta et al. [30] found that honeycomb-patterned specimens exhibited the highest strength. Furthermore, nozzle geometry and diameter significantly affect material performance by influencing void content in printed parts [12].

A survey of the literature reveals that extensive research has been undertaken on the thermal, mechanical, and microstructural properties of ABS, PLA, and PETG parts fabricated via FDM. However, systematic studies investigating the combined effects of material type, infill density, and infill pattern on tensile behavior remain limited.

This work involved the fabrication of tensile specimens using FDM, considering these characteristics. The influence of material type, infill density, and infill pattern on tensile strength, elongation, and elastic modulus was investigated experimentally, and the relative influence of each parameter was analyzed statistically using ANOVA.

2. MATERIALS AND METHODS

In this study, Elas 3D brand ABS, PETG, and PLA filaments were used in the fabrication. To distinguish between the types of filaments, gray, black, and pastel purple colors were selected, respectively. The tensile specimens were designed according to the ISO 527-2 Type 1A standard, with an overall length of approximately 170 mm, a gauge length of 80 mm, a narrow section width of 10 mm, and a thickness of 4 mm.

For the production of the tensile specimens, a Creality K1 high-speed 3D printer was used, offering an acceleration of 20,000 mm/s² and a printing speed of 600 mm/s, capable of producing objects with a build volume of 220 × 220 × 250 mm^3. The Orca Slicer software was employed for slicing the models for 3D printing, and auxiliary G-codes were generated using the printer settings listed in Table 1. The production process was initiated based on the designs corresponding to the patterns and infill ratios shown in Figure 1. The specimens were produced with two samples for each combination of infill density, infill pattern, and filament type, resulting in a total of 54 tensile specimens (Figure 2).

TABLE I
3D PRINTER SETTINGS

Printer	Creality K1 High Speed
Slicing Software	Orca Slicer
Printing Temperature (°C)	PLA:210, PETG:250, ABS:260
Build Plate Temperature (°C)	PLA:55, PETG:80, ABS:100
Infill Pattern	Triangle, Honeycomb, Rectilinear
Infill Density (%)	15, 30, 45
Layer Height (mm)	0,2
Print Speed (mm/s)	300
Number of Wall Lines	4
Top/Bottom Thickness (mm)	1mm



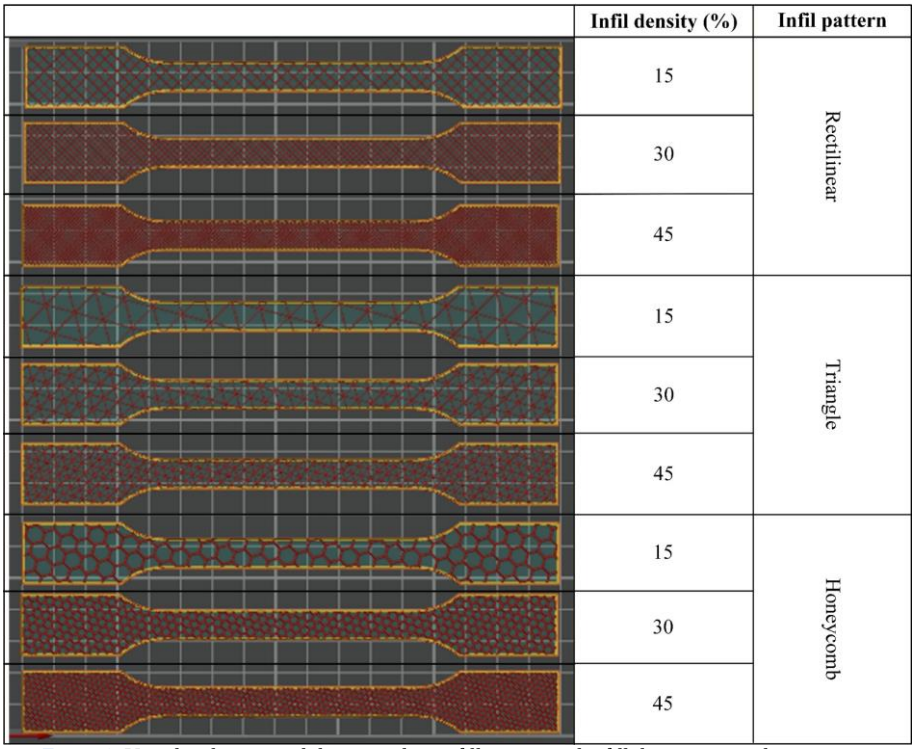


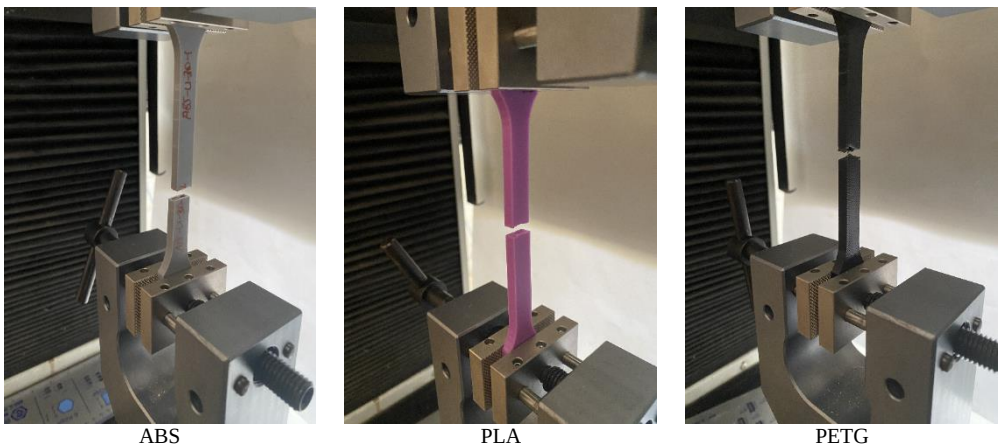
Figure 1. Visual and numerical data regarding infill pattern and infill density in tensile specimens



PETG PLA ABS

Figure 2. Tensile specimens obtained by 3D printing

The use of two specimens per condition (n = 2) was selected to maintain experimental feasibility while enabling the evaluation of a relatively wide parameter space consisting of three filament materials, three infill densities, and three infill patterns. This experimental design resulted in 27 parameter combinations and a total of 54 tensile specimens.



ABS PLA PETG

Figure 3. Tensile testing of specimens fabricated from ABS, PLA, and PETG

Although a larger number of repetitions would improve statistical confidence and allow a more detailed assessment of within-condition variability, the primary objective of this study was to identify comparative trends and the relative influence of process parameters using ANOVA rather than to determine absolute mechanical properties with high statistical precision. All specimens were therefore produced under identical printing conditions and tested using the same experimental setup in order to minimize process-induced variability. Nevertheless, the limited number of repetitions should be considered when interpreting the results, and future studies with larger sample sizes could further improve the statistical robustness of the findings.

The infill density range of 15–45% was selected to represent commonly used levels in practical FDM applications, where weight reduction, material efficiency, and printing time are critical design considerations. Fully solid specimens (100% infill) were intentionally excluded, as they are less representative of lightweight design strategies and would limit the evaluation of density-normalized (specific) mechanical performance. The selected range also reflects commonly used infill densities in lightweight FDM components, where structural efficiency and reduced material consumption are often prioritized over fully solid parts.

The specimens were tested on a Shimadzu universal testing machine with a 5 kN load and a 1 mm/s cross head speed. Images of the experimental setup are shown in Figure 3. The data obtained during the test were recorded on the machine's computer, and tensile strength and modulus of elasticity were calculated using these data. Additionally, ANOVA analysis was applied to identify the effects of the parameters on tensile strength, elongation, and modulus of elasticity.

To assess the performance of the mechanical properties on a per-weight basis, the effective densities of the specimens were calculated using their theoretical volume and measured mass, ensuring that internal voids due to infill density variations were realistically captured. Specific tensile strength and specific modulus values were then re-analyzed through ANOVA to evaluate the effects of material type, infill density, and infill pattern. The results showed that, beyond the absolute mechanical properties, the weight-specific structural efficiency is also influenced by production parameters, offering additional criteria for optimizing FDM-fabricated components.

3. EXPERIMENTAL RESULTS AND DISCUSSION

The tensile test results of specimens fabricated from ABS with 15%, 30%, and 45% infill densities and rectilinear, triangular, and honeycomb infill patterns are given in Figure 4 in terms of tensile strength, elongation, and modulus of elasticity.

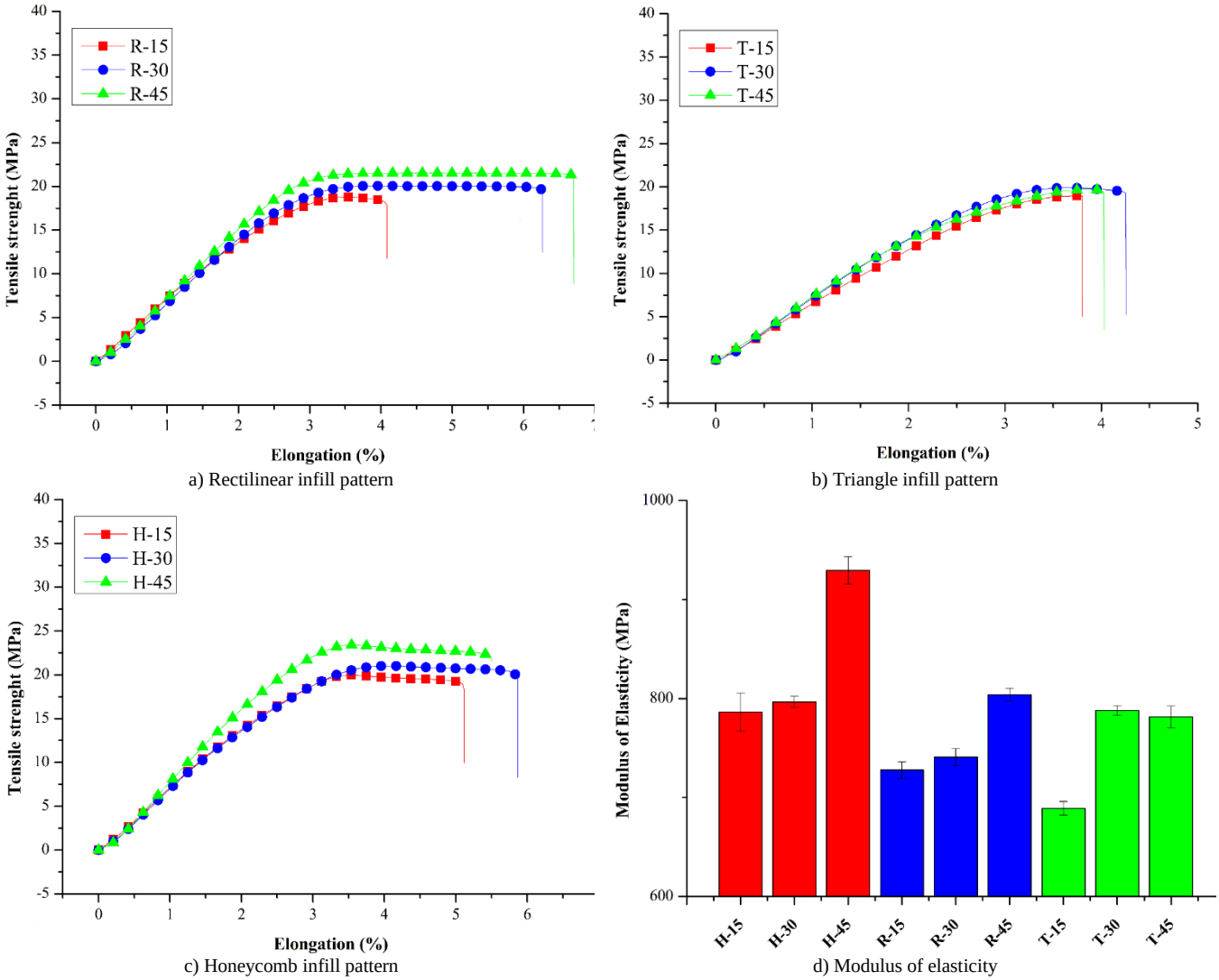


Figure 4. Tensile strength, elongation, and modulus of elasticity of ABS specimens

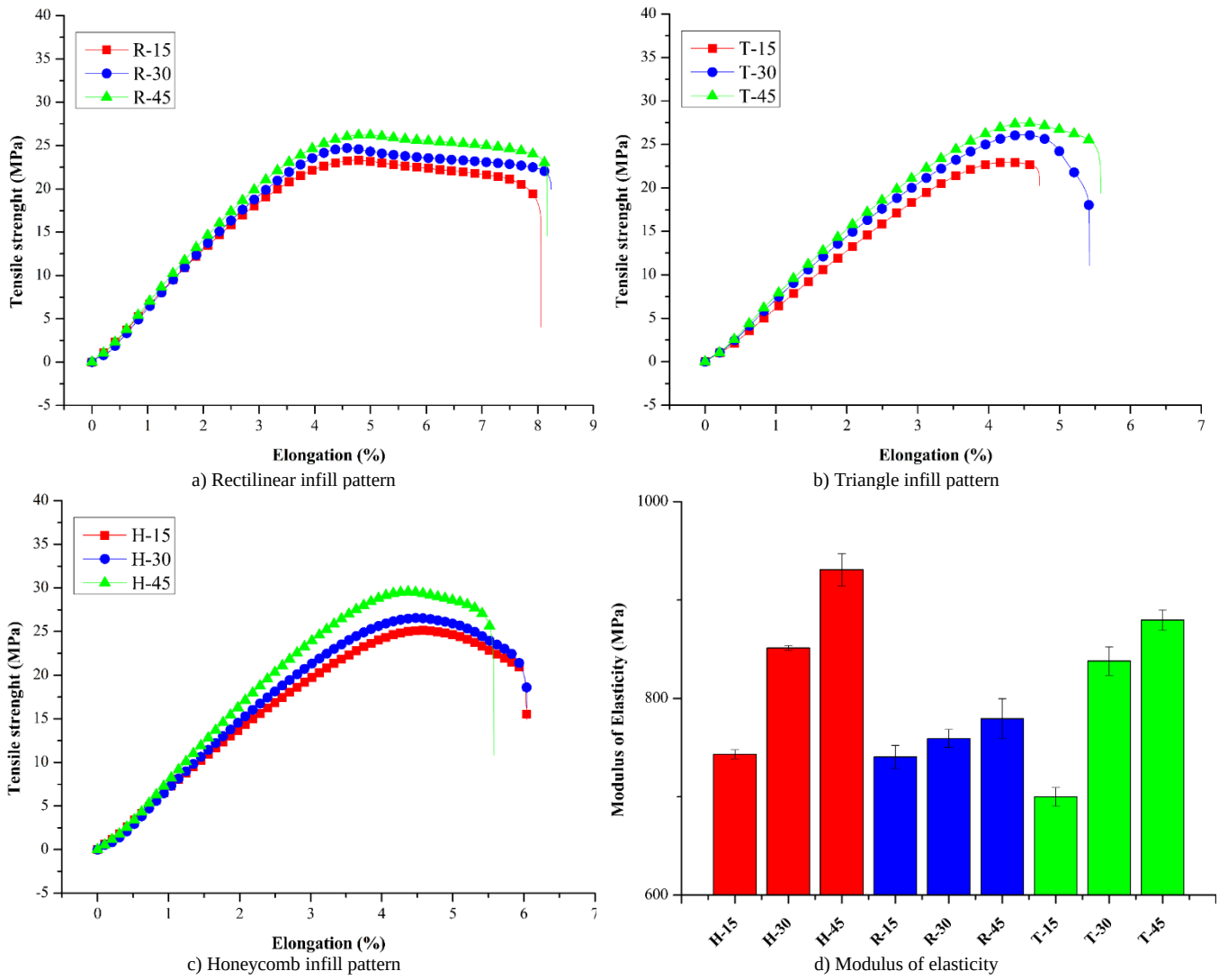
In specimens fabricated from ABS filaments, Figure 4a shows that both tensile strength and elongation increase via higher infill density for the rectilinear infill pattern. The minimum tensile strength and elongation in the rectilinear pattern were measured as 18.78 MPa and 4.09% at 15% infill density, while the maximum values were 21.54 MPa and 6.71% at 45% infill density. In Figure 4b, for the triangular infill pattern, increasing the infill density from 15% to 30% led to an increase in tensile strength from 18.96 MPa to 19.59 MPa and elongation from 3.81% to 5.53%. However, at 45% infill density, both tensile strength and elongation decreased slightly, measured as 18.52 MPa and 4.15%, respectively. For the honeycomb infill pattern in Figure 4c, increasing the infill density generally enhanced both tensile strength and elongation. Tensile strength and elongation were maximum at 45% infill density with values of 23.41 MPa and 5.87%, while the lowest values were obtained at 15% infill density with 19.98 MPa and 5.11%.

Overall, across all infill patterns and densities, tensile strength ranged from 18.78 to 23.41 MPa, while elongation varied between 4.09% and 6.71%, with the highest values observed for the honeycomb infill pattern. Examination of the modulus of elasticity graphs in Figure 4d indicates that both infill pattern and infill density have a significant effect. Increasing the infill density led to higher modulus of elasticity values. The maximum modulus of elasticity, 929.42 MPa, was measured for the honeycomb pattern at 45% infill density, whereas the minimum, 688.92 MPa, was recorded for the triangular pattern at 15% infill density.

Literature studies indicate that infill density is one of the most important parameters influencing the mechanical properties of FDM-fabricated parts. This is because increasing the infill density eliminates internal voids, thereby making the part stiffer and enlarging the load-bearing cross-sectional area [5,31].

Infill pattern, on the other hand, determines the arrangement of internal voids and thus influences the part's response to stress. It has been reported that a hexagonal void structure improves overall mechanical performance, as the hexagonal geometry reduces localized stress concentrations, thereby increasing yield stress and tensile strength [6]. Ali et al. [32] also reported that ABS specimens with a Gyroid infill pattern exhibited the highest compressive strength and ultimate tensile stress.

The tensile strength, elongation and modulus of elasticity values obtained as a result of tensile tests of rectilinear, triangular and honeycomb filler patterned samples produced from PETG filaments with 15%, 30% and 45% filler ratios are given in Figure 5.



a) Rectilinear infill pattern

b) Triangle infill pattern

c) Honeycomb infill pattern

d) Modulus of elasticity

Figure 5. Tensile strength, elongation, and modulus of elasticity of PETG specimens

Based on the data presented in Figure 5, the tensile strengths of the specimens produced from PETG filaments were obtained in the range of 23.30–29.57 MPa, elongation in the range of 4.72–8.24%, and the modulus of elasticity in the

range of 740.36–930.93 MPa. Similar to the specimens produced with ABS filaments, an increase in infill density improved the mechanical properties of the PETG specimens, and the highest mechanical performance was obtained from honeycomb patterned specimens with 45% infill density. This pattern was followed by triangular and rectilinear infill patterns, respectively. Overall, the obtained values were higher than those achieved with ABS filaments. Mishra et al. [33] reported that the ductility of PETG is higher than that of ABS and ABS/PETG blends. Khan et al. [29] also demonstrated that high mechanical properties are achieved when high layer thickness and high infill density, while low infill density leads to the formation of micro-voids, gaps, delamination, and peel-like structures, thereby reducing tensile strength.

The primary way to enhance the mechanical performance of parts produced by FDM is to minimize voids and porosity within the printed structure [34,35]. Reducing the porosity increases the amount of load-bearing material and the inter-filament contact area, thereby improving tensile strength and modulus of elasticity [35]. Increasing infill density enhances the amount of material within the part and reinforces the load-carrying capacity of the structure [29, 36]. Valvez et al. [36] stated that an infill density of 100% is the most critical factor in maximizing the mechanical properties of PETG and PETG composites.

The tensile test results of the PLA specimens are given in Figure 6 in terms of tensile strength, elongation, and modulus of elasticity. It can be seen that the mechanical properties of the specimens produced with PLA filament show trends similar to those of specimens produced with ABS and PETG filaments. The highest tensile strength and modulus of elasticity were obtained from the specimen with a honeycomb pattern and 45% infill density, with values of 34.95 MPa and 1380.66 MPa, respectively. The lowest tensile strength and modulus of elasticity were observed in the specimen with a rectilinear infill pattern. For the PLA specimens, tensile strength ranged from 27.50 to 34.95 MPa, elongation at break ranged from 3.31% to 4.38%, and the modulus of elasticity ranged from 1077 to 1380.66 MPa.

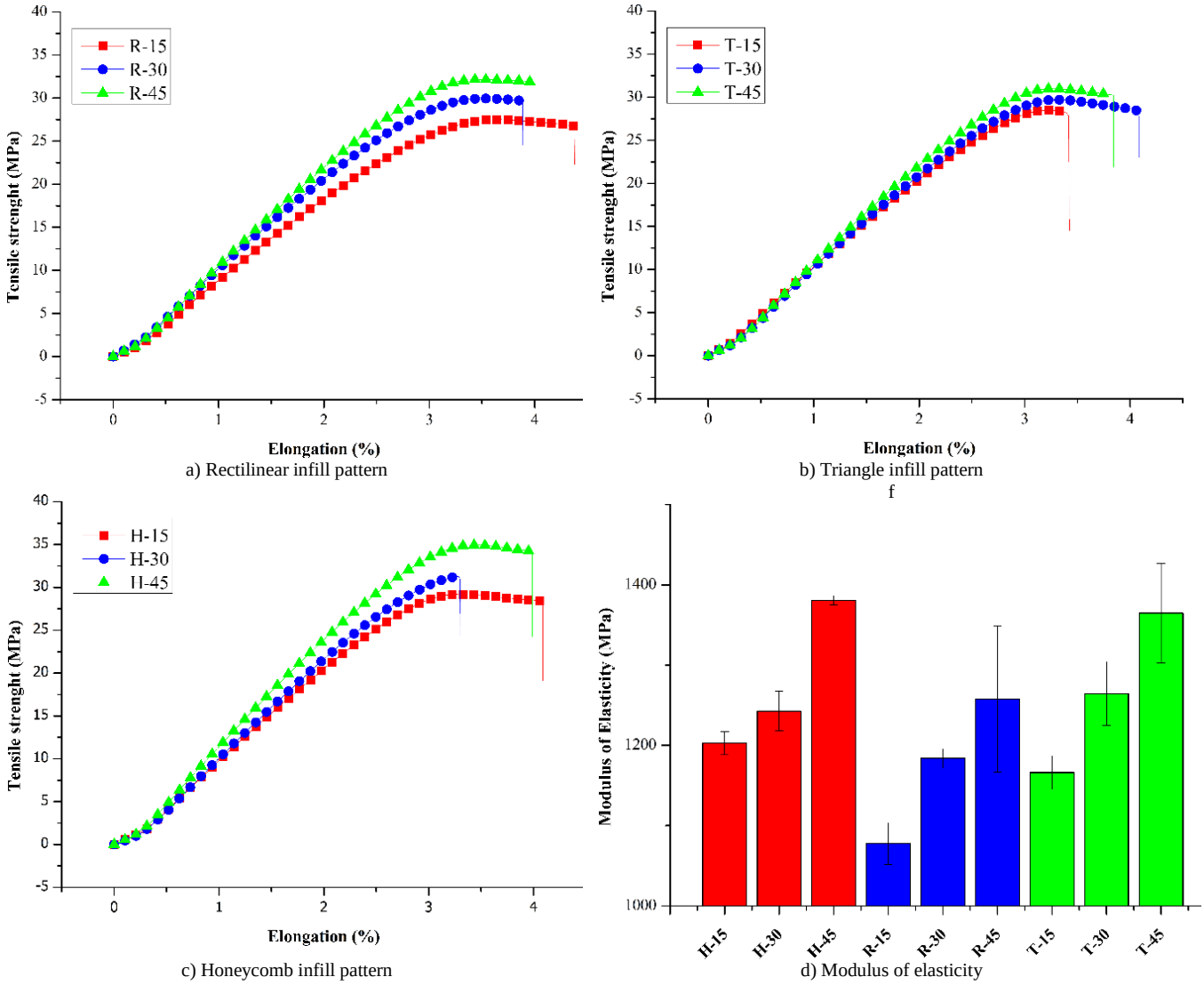


Figure 6. Tensile strength, elongation, and modulus of elasticity of PLA specimens

The PLA specimens exhibited higher tensile strength and modulus of elasticity compared to the ABS and PETG specimens, while showing lower ductility. In a similar study, Güdür et al. [37] produced PLA, ABS, and PETG polymers using the FDM method with different lattice designs, and reported that in the gyroid lattice structure, PETG exhibited maximum deformation, whereas PLA achieved maximum tensile strength. Sepahi et al. [38] investigated the effects of five different raster angles on tensile strength, elongation, and modulus of elasticity, and indicated that PETG showed the

highest elongation, while PLA demonstrated the highest tensile strength and modulus of elasticity. Furthermore, in the study conducted by Ekrem and Yılmaz [13], the maximum stress values of specimens produced with PLA, PETG, and ABS filaments were reported as 48 MPa for PLA, 51.3 MPa for PETG, and 42.8 MPa for ABS, respectively.

The effects of filament material type, infill pattern and density on tensile strength, elongation and modulus of elasticity were analyzed using ANOVA, and the results are given in Table 2.

The filament type was the process parameter contributing most significantly to tensile strength, elongation, and modulus of elasticity. The contribution ratios of this parameter to tensile strength, elongation, and modulus of elasticity were determined as 83.64%, 54.95%, and 88.51%, respectively, indicating a particularly dominant role in tensile strength and modulus of elasticity. The infill pattern contributed 4.11% and 2.60% to tensile strength and modulus of elasticity, respectively, while its contribution to elongation was highest at 18.67%. Infill density provided a higher contribution than the infill pattern to tensile strength and modulus of elasticity, but it was the parameter with the lowest contribution to elongation.

TABLE II

ANOVA ANALYSIS CONDUCTED ON THE ABSOLUTE VALUES OF THE MECHANICAL PROPERTIES

Tensile Strength							
Source	*DF*	*Seq SS*	*Contribution*	*Adj SS*	*Adj MS*	*F-Value*	*P-Value*
Filament Materials	2	478.34	83.64%	478.27	239.137	248.06	0.0000
Infill Pattern	2	23.49	4.11%	23.48	11.738	12.18	0.0003
Infill Density (%)	2	50.82	8.89%	50.81	25.407	26.35	0.0000
Error	20	19.25	3.37%	19.28	0.964		
Total	26	571.91	100.00%				
S 0.981852			R-sq 96.63%			R-sq(adj) 95.62%	
Elongation (%)							
Source	*DF*	*Seq SS*	*Contribution*	*Adj SS*	*Adj MS*	*F-Value*	*P-Value*
Filament Materials	2	29.111	54.95%	29.111	14.5555	23.28	0.0000
Infill Pattern	2	9.891	18.67%	9.891	4.9456	7.91	0.0029
Infill Density (%)	2	1.477	2.79%	1.477	0.7383	1.18	0.3275
Error	20	12.503	23.60%	12.503	0.6251		
Total	26	52.981	100.00%				
S 0.790654			R-sq 76.40%			R-sq(adj) 69.32%	
Modulus of Elasticity							
Source	*DF*	*Seq SS*	*Contribution*	*Adj SS*	*Adj MS*	*F-Value*	*P-Value*
Filament Materials	2	1191624	88.51%	1191626	595813	404.08	0.0000
Infill Pattern	2	35011	2.60%	35009	17504	11.87	0.0004
Infill Density (%)	2	90256	6.70%	90256	45128	30.61	0.0000
Error	20	29490	2.19%	29490	1474		
Total	26	1346381	100.00%				
S 38.3989			R-sq 97.81%			R-sq(adj) 97.15%	

The studies reported in the literature are consistent with the mechanical behavior trends observed in this study. Gonabadi et al. [39] reported that different infill patterns had minimal effects on mechanical properties. Benamira et al. [40] investigated the main and interaction effects of layer thickness and print orientation at 100% and 40% infill densities. They found that at 100% infill density, layer thickness had a significant effect on the modulus of elasticity, while at 40% infill density, both layer thickness and print orientation had significant effects on tensile strength and elongation.

For the purpose of evaluating mechanical performance on a weight basis, the densities of ABS, PETG, and PLA materials were determined as 1.04, 1.25, and 1.26 g/cm^3, respectively, based on the length and mass of the filaments used. The effective density was then calculated using the nominal cross-sectional area of the tested region. Based on these effective density values, the specific strength and specific modulus of the specimens were obtained, and the results are presented in Table 3.

Specific strength measures the load-bearing capacity per unit weight of the specimens. According to the obtained results, although the absolute strength of all materials increases with increasing infill density, the performance per unit weight decreases due to the increased density. In this context, specimens with 15% infill generally exhibited the highest specific strength, while those with 30% and 45% infill showed lower values. Similarly, the specific modulus reflects the stiffness provided by the structure per unit weight. Specimens with 15% infill generally demonstrated higher specific modulus values, followed by those with 30% and 45% infill densities.

In the material-based evaluation, the higher densities of PLA and PETG compared to ABS resulted in lower specific strength and specific modulus values. For PLA and ABS specimens, those with a triangular infill pattern and 45% infill density exhibited the lowest specific strength, whereas for PETG, the lowest value was observed in the specimen with a rectilinear infill pattern.

On the other hand, although ABS specimens exhibited lower absolute strength, they demonstrated comparable performance to the other materials in terms of strength per unit weight. Regarding specific modulus, the difference between ABS and PLA was reduced, and ABS provided higher stiffness per unit weight compared to PETG.

An ANOVA analysis was conducted to evaluate in detail the effects of the manufacturing parameters on specific tensile strength and specific modulus, and the results are given in Table 4.

When the specific tensile strength results in Table 4 were examined, it was seen that the effect of the filament material decreased from 83.64% to 62.64%, and the infill pattern decreased from 4.11% to 1.29%. In contrast, the effect of infill density, previously 8.89%, increased to 28.17%, becoming a strong factor. The infill pattern variable was determined to lose statistical significance due to a p=0.22. Although the filament material still had the largest effect in the normalized data, the effect of infill density increased significantly, indicating that the difference decreased with normalization.

TABLE III
DATA OBTAINED FROM EXPERIMENTS AND VALUES NORMALIZED ACCORDING TO EFFECTIVE DENSITY

Material	Infill Pattern - density	Effective density (g/cm^3)	Ultimate Tensile Strength (MPa)	Modulus of Elasticity (MPa)	Elongation (%)	Specific Strength (MPa×cm^3/g)	Specific Modulus (MPa×cm^3/g)
ABS	R-15	0.59	18.78	727.69	4.09	31.83	1233.38
ABS	R-30	0.68	20.09	740.73	6.27	29.76	1097.37
ABS	R-45	0.76	21.54	803.75	6.71	28.44	1061.06
ABS	T-15	0.59	18.96	688.92	3.81	32.41	1177.64
ABS	T-30	0.67	19.59	787.83	5.53	29.24	1175.86
ABS	T-45	0.76	18.22	781.52	4.15	24.14	1035.13
ABS	H-15	0.61	19.98	786.26	5.12	32.76	1288.96
ABS	H-30	0.71	21.02	796.60	5.87	29.61	1121.98
ABS	H-45	0.80	23.41	929.42	5.51	29.17	1158.16
PETG	R-15	0.71	23.30	740.36	8.06	32.81	1042.75
PETG	R-30	0.81	24.72	759.35	8.24	30.51	937.47
PETG	R-45	0.91	26.24	779.36	8.17	28.83	856.43
PETG	T-15	0.70	22.95	700.04	4.72	32.67	996.49
PETG	T-30	0.81	26.12	838.02	5.42	32.44	1041.02
PETG	T-45	0.91	27.47	879.56	5.58	30.27	969.21
PETG	H-15	0.73	25.15	743.27	6.04	34.34	1014.71
PETG	H-30	0.86	26.56	851.22	6.05	31.07	995.58
PETG	H-45	0.97	29.57	930.93	5.58	30.64	964.69
PLA	R-15	0.74	27.50	1077.44	4.38	37.42	1465.91
PLA	R-30	0.84	29.96	1183.77	3.89	35.67	1409.25
PLA	R-45	0.95	32.16	1257.52	3.98	34.03	1330.71
PLA	T-15	0.73	28.49	1166.17	3.42	39.16	1602.98
PLA	T-30	0.84	29.71	1264.62	4.08	35.58	1514.52
PLA	T-45	0.94	30.99	1364.66	3.85	32.88	1447.91
PLA	H-15	0.76	29.20	1202.64	4.09	38.42	1582.42
PLA	H-30	0.89	31.29	1242.78	3.31	35.26	1400.31
PLA	H-45	1.00	34.95	1380.66	3.99	34.95	1380.66

TABLE IV
ANALYSIS OF VARIANCE (ANOVA) CONDUCTED ON SPECIFIC (NORMALIZED) VALUES

Specific Tensile Strength

Source	*DF*	*Seq SS*	*Contribution*	*Adj SS*	*Adj MS*	*F-Value*	*P-Value*
Filament Materials	2	184.671	62.64%	184.671	92.336	79.23	0.0000
Infill Pattern	2	3.810	1.29%	3.810	1.905	1.63	0.2200
Infill Density (%)	2	83.043	28.17%	83.043	41.522	35.63	0.0000
Error	20	23.309	7.91%	23.309	1.165		
Total	26	294.834	100.00%				
S 1,7956			R-sq 92,09%		R-sq(adj) 89,72%		

Specific Modulus

Source	*DF*	*Seq SS*	*Contribution*	*Adj SS*	*Adj MS*	*F-Value*	*P-Value*
Filament Materials	2	1064147	87.87%	1064147	532073	225.40	0.0000
Infill Pattern	2	18661	1.54%	18661	9330	3.95	0.0358
Infill Density (%)	2	81086	6.70%	81086	40543	17.18	0.0000
Error	20	47212	3.90%	47212	2361		
Total	26	1211105					
S 48,5858			R-sq 96,10%		R-sq(adj) 94,93%		

When the specific module results are examined, it is seen that the effect of normalization is much more limited. While the effect of filament material type decreased from 88.51% to 87.87%, the effect of infill pattern decreased from 2.60% to 1.54%, and the effect of infill density remained unchanged at 6.70%. All three parameters were found to be statistically significant ($p<0.05$). These results indicate that the effects of the variables on specific modulus remained nearly the same after normalization, and weight did not significantly affect the specific modulus.

4. CONCLUSION

In this study, the tensile behavior of FDM-printed ABS, PETG, and PLA specimens manufactured with different infill densities (15%, 30%, and 45%) and infill patterns (honeycomb, triangular, and rectilinear) was experimentally investigated. The mechanical performance in terms of tensile strength, elongation, and elastic modulus was evaluated, and the relative influence of process parameters was quantified using ANOVA.

Overall, increasing the infill density resulted in improved tensile properties for all materials. Among the investigated infill geometries, the honeycomb pattern generally provided higher tensile strength and elastic modulus. Material type was identified as the most influential parameter governing mechanical performance. PLA specimens exhibited the highest tensile strength and stiffness but showed limited elongation, whereas PETG demonstrated more ductile behavior with the highest elongation values. ABS samples displayed lower absolute mechanical properties; however, their lower density enabled more competitive performance when evaluated on a specific (weight-normalized) basis.

The analysis of normalized mechanical properties highlighted that infill density plays a more pronounced role in specific tensile strength, thereby reducing the dominance of filament type. These findings indicate that the mechanical evaluation of FDM components should not be limited to absolute property values but should also consider performance per unit weight, particularly for lightweight structural applications.

From an industrial perspective, the results provide useful guidance for the design of lightweight FDM components. In many applications, reducing material usage and printing time while maintaining sufficient mechanical performance is essential. The findings indicate that appropriate combinations of filament type, infill density, and infill pattern can be selected to balance mechanical performance with manufacturing efficiency and material cost.

This study focused exclusively on tensile loading under quasi-static conditions and considered a limited range of infill densities and patterns. Other critical factors such as raster angle, layer thickness, build orientation, and environmental effects were not addressed. In addition, the results are specific to the selected filament brands and printing parameters. Future studies could extend the analysis to different loading modes (e.g., flexural and impact), broader process windows, and long-term performance under thermal or environmental aging to provide a more comprehensive assessment of FDM-printed components.

REFERENCES

[1] Q. He, T. Tang, Y. Zeng, N. Iradukunda, B. Bethers, X. Li, & Y. Yang, 'Review on 3D printing of bioinspired structures for surface/interface applications', in *Advanced Functional Materials*, vol. 34, no. 11, 2309323, 2024. doi: 10.1002/adfm.202309323.

[2] V. D. Sagias, K. I. Giannakopoulos, and C. Stergiou, 'Mechanical properties of 3D printed polymer specimens', in *Procedia Structural Integrity*, Elsevier B.V., 2018, pp. 85–90. doi: 10.1016/j.prostr.2018.09.013.

[3] M. Azadi, A. Dadashi, S. Dezianian, M. Kianifar, S. Torkaman, and M. Chiyani, 'High-cycle bending fatigue properties of additive-manufactured ABS and PLA polymers fabricated by fused deposition modeling 3D-printing', *Forces in Mechanics*, vol. 3, Sep. 2021, doi: 10.1016/j.finmec.2021.100016.

[4] R. T. Mushtaq *et al.*, 'Multi-objective optimization of laser polishing parameters for enhanced mechanical properties, sustainability, and surface finish of 3D-Printed industrial ABS polymers using response surface methodology (RSM)', *Journal of Materials Research and Technology*, vol. 29, pp. 3168–3184, Mar. 2024, doi: 10.1016/j.jmrt.2024.02.023.

[5] M. Algarni and S. Ghazali, 'Comparative study of the sensitivity of PLA, ABS, PEEK, and PETG's mechanical properties to FDM printing process parameters', *Crystals (Basel)*, vol. 11, no. 8, Aug. 2021, doi: 10.3390/cryst11080995.

[6] Y. S. Perera, O. Exley, S. A. V. Dananjaya, N. Hansika, and C. Abeykoon, 'Investigation of the mechanical properties of 3D printed hollow parts with finite element analysis', *Journal of Materials Research and Technology*, vol. 36, pp. 8826–8839, May 2025, doi: 10.1016/j.jmrt.2025.05.104.

[7] F. Kartal and A. Kaptan, 'Prediction and optimization of tensile strength values of 3D printed PLA components with RSM, ANOVA and ANN analysis', vol. 15, no. 1, p. 2025, doi: 10.36222/ejt.1561857.

[8] M. H. Boztepe, 'A study on the mechanical properties of PLA+ samples manufactured using 3D printing with different raster angles', *Kahramanmaras Sutcu Imam University Journal of Engineering Sciences*, vol. 28, no. 2, pp. 923–932, 2025.

[9] P. Anerao, A. Kulkarni, Y. Munde, and N. Kharate, 'A comparative study of machine learning techniques for predicting mechanical properties of fused deposition modelling (FDM)-based 3D-printed wood/PLA biocomposite', *Mechanics of Advanced Composite Structures*, vol. 12, no. 2, pp. 261–270, Aug. 2025, doi: 10.22075/macs.2024.33776.1638.

[10] K. V. Durga Rajesh, N. Ganesh, S. Yaswanth Kalyan Reddy, H. Mishra, and T. M. V. P. S. Teja Naidu, 'Experimental research on the mechanical characteristics of fused deposition modelled ABS, PLA and PETG specimens printed in 3D', *Mater Today Proc*, Jul. 2023, doi: 10.1016/j.matpr.2023.06.343.

[11] N. Vidakis, M. Petousis, E. Velidakis, M. Liebscher, V. Mechtcherine, and L. Tzounis, 'On the strain rate sensitivity of fused filament fabrication (Fff) processed PLA, ABS, PETG, PA6, and PP thermoplastic polymers', *Polymers (Basel)*, vol. 12, no. 12, pp. 1–15, Dec. 2020, doi: 10.3390/polym12122924.

[12] T. Khan *et al.*, 'Recent developments in improving the fracture toughness of 3D-printed fiber-reinforced polymer composites', Aug. 15, 2024, *Elsevier Ltd*. doi: 10.1016/j.compositesb.2024.111622.

[13] M. Ekrem ve M. Yılmaz, 'Yüksek hızlı 3B yazıcıda basılmış PLA, PETG ve ABS numunelerin mekanik özellikleri', vol. 7, no. 1, pp. 2667–7989, doi: 10.47112/neufmbd.2024.83.

[14] M. Kopar, M. Sömer, and M. B. Çalışkan, 'Experimental investigation of the effect of raster angle and printing speed on mechanical performance and fracture behavior of ABS material produced by FFF technology', *Fırat Üniversitesi Mühendislik Bilimleri Dergisi*, vol. 37, no. 2, pp. 737–746, Sep. 2025, doi: 10.35234/fumbd.1700589.

[15] K. Almansoori and S. Pervaiz, 'Effect of layer height, print speed and cell geometry on mechanical properties of marble PLA based 3D printed parts', *Smart Materials in Manufacturing*, vol. 1, Jan. 2023, doi: 10.1016/j.smmf.2023.100023.

[16] M. H. Hsueh *et al.*, 'Effect of printing parameters on the thermal and mechanical properties of 3d-printed pla and petg, using fused deposition modeling', *Polymers (Basel)*, vol. 13, no. 11, Jun. 2021, doi: 10.3390/polym13111758.

[17] M. H. Boztepe (2025). Investigation of Tensile Strength in 3D Printed PLA+ Samples: Influence of Raster Angle and Infill Density. Çukurova Üniversitesi Mühendislik Fakültesi Dergisi, 40(4), 937-948, doi: 10.21605/cukurovaumfd.1652812

[18] M. H. Boztepe and M. Haskul (2026). Mechanical Characterization of PLA+ Specimens with Different Geometries Using Experimental and Numerical Methods. Polymers, 18(2), 243, doi: 10.3390/polym18020243

[19] Kartal, F., & Kaptan, A. (2025). Prediction and Optimization of Tensile Strength Values of 3D Printed PLA Components with RSM, ANOVA and ANN Analysis. European Journal of Technique (EJT), 15(1), 51-60, doi: 10.36222/ejt.1561857.

[20] B. Stecuła, J. Sitko, K. Stecuła, M. Witkowski, and B. Orzeł, 'Comparison of the strength of popular thermoplastic materials used in 3D printing – PLA, ABS and PET-G', *Combustion Engines*, vol. 199, no. 4, pp. 97–103, 2024, doi: 10.19206/CE-189386.

[21] R. Mendenhall and B. Eslami, 'Experimental ınvestigation on effect of temperature on FDM 3D printing polymers: ABS, PETG, and PLA', *Applied Sciences (Switzerland)*, vol. 13, no. 20, Oct. 2023, doi: 10.3390/app132011503.

[22] O. Tunçel, 'The influence of the raster angle on the dimensional accuracy of FDM-printed PLA, PETG, and ABS tensile specimens', *European Mechanical Science*, vol. 8, no. 1, pp. 11–18, Mar. 2024, doi: 10.26701/ems.1392387.

[23] H. Gonabadi, S. F. Hosseini, Y. Chen, and S. Bull, 'Size effects of voids on the mechanical properties of 3D printed parts', *International Journal of Advanced Manufacturing Technology*, vol. 132, no. 11–12, pp. 5439–5456, Jun. 2024, doi: 10.1007/s00170-024-13683-9.

[24] P. Wang *et al.*, 'Preparation of short CF/GF reinforced PEEK composite filaments and their comprehensive properties evaluation for FDM-3D printing', *Compos B Eng*, vol. 198, Oct. 2020, doi: 10.1016/j.compositesb.2020.108175.

[25] B. G. Çakan, 'Effects of raster angle on tensile and surface roughness properties of various FDM filaments', *Journal of Mechanical Science and Technology*, vol. 35, no. 8, pp. 3347–3353, Aug. 2021, doi: 10.1007/s12206-021-0708-8.

[26] R. F. Faidallah, M. M. Hanon, V. Vashist, A. Habib, Z. Szakál, and I. Oldal, 'Effect of different standard geometry shapes on the tensile properties of 3D-printed polymer', *Polymers (Basel)*, vol. 15, no. 14, Jul. 2023, doi: 10.3390/polym15143029.

[27] N. Vinoth Babu *et al.*, 'Influence of slicing parameters on surface quality and mechanical properties of 3D-printed CF/PLA composites fabricated by FDM technique', *Materials Technology*, vol. 37, no. 9, pp. 1008–1025, 2022, doi: 10.1080/10667857.2021.1915056.

[28] J. R. C. Dizon, A. H. Espera, Q. Chen, and R. C. Advincula, 'Mechanical characterization of 3D-printed polymers', Mar. 01, 2018, *Elsevier B.V.* doi: 10.1016/j.addma.2017.12.002.

[29] I. Khan *et al.*, 'Parametric investigation and optimisation of mechanical properties of thick tri-material based composite of PLA-PETG-ABS 3D-printed using fused filament fabrication', *Composites Part C: Open Access*, vol. 12, Oct. 2023, doi: 10.1016/j.jcomc.2023.100392.

[30] T. Galeta, P. Raos, J. Stojšić, and I. Pakši, 'Influence of structure on mechanical properties of 3D printed objects', in *Procedia Engineering*, Elsevier Ltd, 2016, pp. 100–104. doi: 10.1016/j.proeng.2016.06.644.

[31] Ö. Çerlek, K. Han, Y. Akin, and Ö. Seçgin, 'Experimental Investigation of Parameters Affecting the Tensile Strength of Silicone-Filled 3D Printed ABS Products', *J Mater Eng Perform*, vol. 34, no. 11, pp. 9627–9636, Jun. 2025, doi: 10.1007/s11665-024-10498-3.

[32] H. B. Ali, J. K. Oleiwi, and F. M. Othman, 'Compressive and tensile properties of ABS Material as a Function of 3D printing process parameters', *Revue des Composites et des Materiaux Avances*, vol. 32, no. 3, pp. 117–123, Jun. 2022, doi: 10.18280/rcma.320302.

[33] V. Mishra, D. Veeman, and S. Negi, 'Enhanced tensile strength and fracture toughness of 3D printed PETG/ABS blend for load-bearing application', *J Mater Eng Perform*, Nov. 2025, doi: 10.1007/s11665-025-11208-3.

[34] J. Loskot *et al.*, 'Influence of print speed on the microstructure, morphology, and mechanical properties of 3D-printed PETG products', *Polym Test*, vol. 123, Jun. 2023, doi: 10.1016/j.polymertesting.2023.108055.

[35] A. Özen, B. E. Abali, C. Völlmecke, J. Gerstel, and D. Auhl, 'Exploring the role of manufacturing parameters on microstructure and mechanical properties in fused deposition modeling (FDM) using PETG', *Applied Composite Materials*, vol. 28, no. 6, pp. 1799–1828, Dec. 2021, doi: 10.1007/s10443-021-09940-9.

[36] S. Valvez, A. P. Silva, and P. N. B. Reis, 'Optimization of printing parameters to maximize the mechanical properties of 3D-printed PETG-based parts', *Polymers (Basel)*, vol. 14, no. 13, Jul. 2022, doi: 10.3390/polym14132564.

[37] C. Güdür, T. Türkoğlu, and İ. Eren, 'Effect of lattice design and process parameters on the properties of PLA, ABS and PETG polymers produced by fused deposition modelling', *Journal of Materials and Mechatronics: A*, vol. 4, no. 2, pp. 561–570, Dec. 2023, doi: 10.55546/jmm.1357217.

[38] M. T. Sepahi, H. Abusalma, V. Jovanovic, and H. Eisazadeh, 'Mechanical properties of 3D-printed parts made of polyethylene terephthalate glycol', *J Mater Eng Perform*, vol. 30, no. 9, pp. 6851–6861, Sep. 2021, doi: 10.1007/s11665-021-06032-4.

[39] H. Gonabadi, & A. Yadav, and S. J. Bull, 'The effect of processing parameters on the mechanical characteristics of PLA produced by a 3D FFF printer', doi: 10.1007/s00170-020-06138-4/Published.

[40] M. Benamira, N. Benhassine, A. Ayad, and A. Dekhane, 'Investigation of printing parameters effects on mechanical and failure properties of 3D printed PLA', *Eng Fail Anal*, vol. 148, Jun. 2023, doi: 10.1016/j.engfailanal.2023.107218.

BIOGRAPHIES

İsmail Erhan Kutsal received his BSc degree in the Department of Mechanical Engineering at Atatürk University in 2006. He is currently a lecturer in the Mechanical Program at Sirnak University Vocational School and is pursuing his PhD at Batman University. His research interests include machining, tool wear, 3D printing, and AI-assisted manufacturing processes.

Dr. Serkan Bati is an Assistant Professor in the Department of Mechanical Engineering at Batman University. His research interests focus on coatings, tribology, and the low- and high-velocity impact behavior of fiber-reinforced composites.

Prof. Dr. Yahya Hışman Çelik obtained his BSc degree from the Department of Mechanical Engineering. He is currently a Professor at Batman University, specializing in manufacturing technologies, materials design, and mechanical behavior.